



Cite this: DOI: 10.1039/d0dt03805a

Received 4th November 2020,  
Accepted 21st December 2020

DOI: 10.1039/d0dt03805a

rsc.li/dalton

Cleavage of cluster iron–sulfide bonds in  
cyclophane-coordinated  $\text{Fe}_n\text{S}_m$  complexes†William R. Buratto,<sup>a</sup> Ricardo B. Ferreira,<sup>a</sup> Vincent J. Catalano,<sup>b</sup>  
Ricardo García-Serres<sup>c</sup> and Leslie J. Murray<sup>\*,a</sup>

Reaction of the tri( $\mu$ -sulfido)triiron(III) tris( $\beta$ -diketiminate) cyclophane complex,  $\text{Fe}_3\text{S}_3\text{L}^{\text{Et/Me}}$  (1), or of the di( $\mu$ -sulfido)diiron(III) complex  $\text{Fe}_2\text{S}_2\text{HL}^{\text{Et/Me}}$  (5), with the related tri(bromide)triiron(II) complex  $\text{Fe}_3\text{Br}_3\text{L}^{\text{Et/Me}}$  (2) results in electron and ligand redistribution to yield the mixed-ligand multiiron complexes, including  $\text{Fe}_3\text{Br}_2\text{SL}^{\text{Et/Me}}$  (3) and  $\text{Fe}_2\text{Br}_2\text{SHL}^{\text{Et/Me}}$  (4). The cleavage and redistribution observed in these complexes is reminiscent of necessary Fe–S bond cleavage for substrate activation in nitrogenase enzymes, and provides a new perspective on the lability of Fe–S bonds in FeS clusters.

Iron–sulfur (FeS) clusters are ubiquitous in biological systems and critical for numerous functions including electron transfer and substrate binding and activation. Two common forms of these clusters are the cuboidal [4Fe–4S] cluster and the rhomboid [2Fe–2S] cluster, and the cluster Fe–S bonds generally remain intact during the execution of function. Synthetic FeS cluster chemistry suggests these clusters are thermodynamically preferred structures; for example, the Holm group has reported that  $\text{Fe}_4\text{S}_4$  cubanes remain intact upon treatment with numerous reagents including selenolates, acetyl chloride, and strong acids.<sup>1–3</sup> On the other hand, the Holm and Tatsumi groups have also reported that additional equivalents of external ligands induce scission of Fe–S bonds at the bridging sulfide sites in the 8Fe–8S and 4Fe–4S clusters, respectively, to generate the related 2Fe–2S or 4Fe–4S compounds.<sup>4,5</sup> Although these results demonstrate that Fe–S bonds can be cleaved, to the best of our knowledge, no examples of  $\text{Fe}^{\text{III}}-(\mu\text{-S})$  bond cleavage have been reported to date.

Recently, however, growing evidence points to Fe–( $\mu$ -S) bond cleavage in biological FeS clusters as critical for protein function, with that observed in HydG and the nitrogenase cofactors being noteworthy. For HydG, the proposed mechanism invokes Fe–( $\mu$ -S) bond scission upon reaction of the mature HydG cofactor with the acceptor protein HydF, which effects transfer of the  $\text{Fe}(\text{CO})_2(\text{CN})$  fragment from HydG to HydF.<sup>6</sup> In the nitrogenase enzymes, by contrast, Fe–S bond cleavage is likely reversible with sulfide dissociation observed under catalytic turnover based on X-ray crystallographic data reported by Rees and Einsle and their respective coworkers. Spatzal *et al.* observed Se incorporation at the  $\mu$ -sulfide (or belt sulfide) sites in the iron–molybdenum cofactor (FeMoco) in the enzyme crystallized after catalytic turnover in the presence of selenocyanate, and Spatzal *et al.* also reported crystallographic evidence for substitution of one belt sulfide for a CO donor in the CO inhibited state of the cofactor.<sup>7,8</sup> Similarly, Sippel *et al.* observed replacement of one  $\mu$ -sulfide in the iron–vanadium cofactor (FeVco) in nitrogenase from *A. vinelandii* by light atom donors proposed as dinitrogen derived (Fig. 1).<sup>9</sup> More recently, a crystal structure and anomalous difference Fourier map of an electron-deficient Mo-dependent nitrogenase evidence density consistent with an  $\text{N}_2$  ligand bound to the cofactor in a  $\mu$ -1,2 mode in place of a belt sulfide.<sup>10</sup>

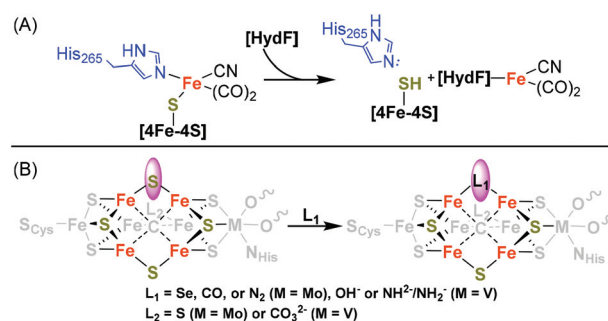


Fig. 1 A bridging sulfide unit is displaced in both the HydG enzyme (A) and nitrogenase enzymes (B).

<sup>a</sup>Department of Chemistry, Center for Catalysis, University of Florida, Gainesville, FL 32611-7200, USA. E-mail: murray@chem.ufl.edu; Tel: +1 352-392-0564

<sup>b</sup>Department of Chemistry, University of Nevada, Reno, Nevada 89557, USA

<sup>c</sup>LCBM/PMB and CEA, iRTSV/CBM/PMB and CNRS, Université Grenoble Alpes, UMR 5249, LCBM/PMB, 38000 Grenoble, France. E-mail: ricardo.garcia@cea.fr

† Electronic supplementary information (ESI) available: Experimental details, additional spectra, X-ray crystallographic information, and additional tables. CCDC 2026540. For ESI and crystallographic data in CIF or other electronic format see DOI: 10.1039/d0dt03805a

## Communication

Spurred by these recent advances, computational and synthetic models have aimed to corroborate the viability of and need for sulfide dissociation as a prerequisite for substrate activation at the nitrogenase cofactors.<sup>11–13</sup> To our knowledge, however, few have sought to explore the lability of Fe–S bonds to yield new structure types with potential for substrate activation. Herein, we report the restructuring of triiron(III) tri( $\mu$ -sulfide) and diiron(III) di( $\mu$ -sulfide) clusters supported by a cyclophane donor upon reaction with complexes lacking sulfide donors. This reaction requires a partner triiron species and leads to redistribution of sulfide ligands and electrons between triiron complexes with no evidence for an outer-sphere reduction step of the  $[\text{Fe}_3\text{S}_3]^{3+}$  complex.

Monitoring the speciation of an equimolar mixture of  $\text{Fe}_3\text{S}_3\text{L}^{\text{Et/Me}}$  (**1**) and  $\text{Fe}_3\text{Br}_3\text{L}^{\text{Et/Me}}$  (**2**) at ambient temperature in  $\text{C}_6\text{D}_6$  by  $^1\text{H-NMR}$  spectroscopy evidence consumption of both **1** and **2** with formation of two major paramagnetic species.<sup>14,15</sup> The first daughter complex from this reaction is the previously reported  $\text{Fe}_3\text{Br}_2\text{SL}^{\text{Et/Me}}$  (**3**) complex and the second is assigned as the di(bromido)( $\mu$ -sulfido)diiron(III) complex  $\text{Fe}_2\text{Br}_2\text{SHL}^{\text{Et/Me}}$  (**4**, *vide infra*, Fig. 2).<sup>16</sup> This initial result provided unequivocal evidence that the  $[\text{3Fe-3S}]^{3+}$  cluster in **1** is unstable with respect to redistribution of ligands and electrons, or scrambling (Fig. 3). Given that **1** and **3** could be readily synthesized from **2** by minor variations to the reaction conditions, we postulated that an initial scrambling-generated triiron species might precede the demetallation reaction leading to **4**. Therefore, we first explored the conditions governing scrambling from **1** and then examined routes to generate **4**.

Scrambling of sulfide donors between **1** and **2** is facile with both complexes consumed within 5 min and even at temperatures as low as  $-40$  °C. Changing other reaction conditions (*viz.* increased temperature, order of addition, reaction time, and solvent) had no effect on product speciation (Fig. S1–7†). Given that reaction of **1** with **2** occurs with redox state changes

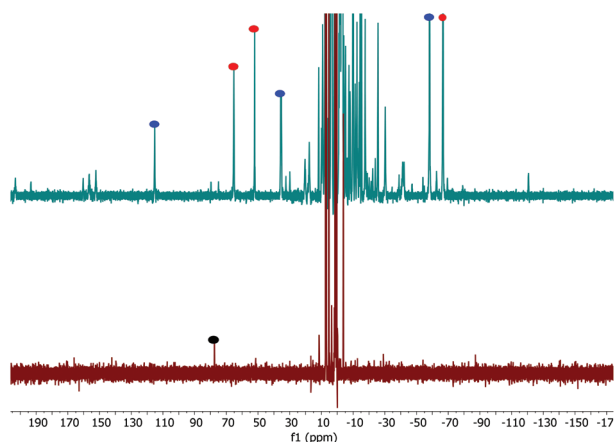


Fig. 2  $^1\text{H-NMR}$  spectra of **1** (bottom) and the product mixture of the scrambling reaction between **1** and **2** (top). The spectra show consumption of **1** (black circle) and formation of **3** and **4** (blue and red circles, respectively). Both spectra were collected in  $\text{C}_6\text{D}_6$  at room temperature.

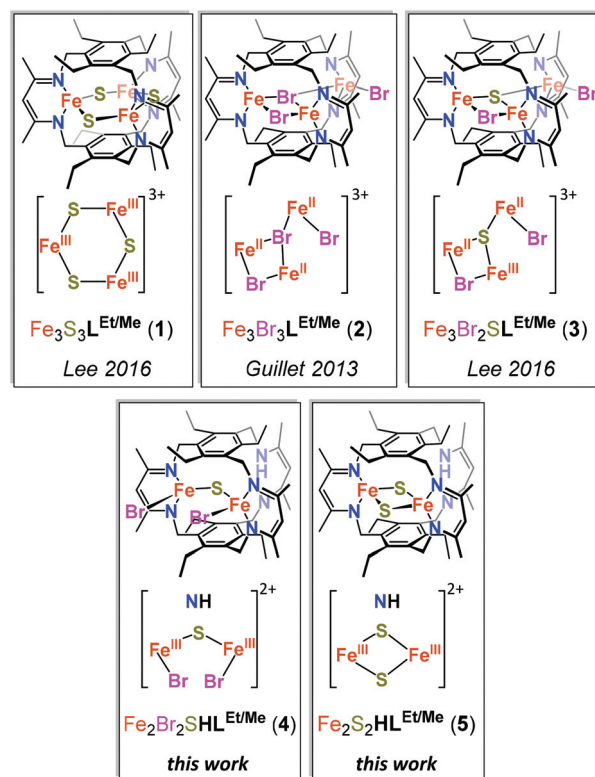


Fig. 3 Structures of the sulfide-containing compounds presented in this work. Note: Provided oxidation states are formal assignments.

for the Fe centers in the respective products (*e.g.*, **1** is all ferric whereas **3** is mixed valent) and demetallation, one might envision that reaction of **1** with salts containing iron(II), bromide, or both would effect a similar reaction. Specifically, demetallation may afford the thermodynamically stable  $[\text{4Fe-4S}]$  or  $[\text{2Fe-2S}]$  clusters supported by halide or solvent donors as by-products with **3** and **4**. Reaction of tetrabutylammonium bromide (TBABr) or  $\text{FeBr}_2$  with  $\text{Fe}_3\text{S}_3\text{L}^{\text{Et/Me}}$  in THF, however, demonstrated no apparent change in the reaction mixture. Examining whether sulfide abstraction would occur concomitant with demetallation, we then attempted to abstract sulfides from **1** by addition of a phosphine (*viz.*  $\text{PPh}_3$ ,  $\text{P}(\text{Mes})_3$ , and  $\text{P}[(2,4,6\text{-trimethoxyphenyl})_3]$  in THF; for these phosphines, we obtained no evidence for formation of the corresponding phosphine sulfide. Of the three possible  $\text{R}_3\text{PS}$  products,  $\text{Ph}_3\text{PS}$  has the strongest calculated P–S bond ( $\sim 70$  kcal mol $^{-1}$ ),<sup>20</sup> providing a lower limit for the Fe–( $\mu$ -S) bond strength in **1**. Although, we cannot rigorously exclude a kinetic barrier for S transfer. We then reacted **1** with the triiron complexes  $\text{Fe}_3\text{H}_3\text{L}^{\text{Et/Me}}$ ,  $\text{Fe}_3(\text{NH}_2)_3\text{L}^{\text{Et/Me}}$ , and  $\text{Fe}_3(\text{OME})_3\text{L}^{\text{Et/Me}}$  to probe whether scrambling requires two cyclophane complexes insofar as exogenous iron(II) and bromide were insufficient (Fig. 4).<sup>17,18</sup> For these three reactions, resonances corresponding to complex **1** in the  $^1\text{H-NMR}$  spectrum decrease and are ultimately undetectable after 18 h, consistent with instability of **1** in the presence of other triiron species. The rate of consumption of **1** in these reactions, however, is notably slower

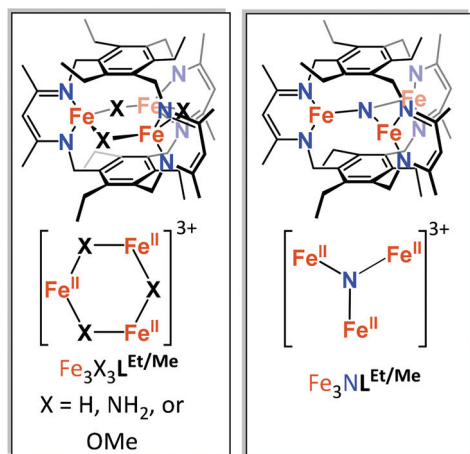
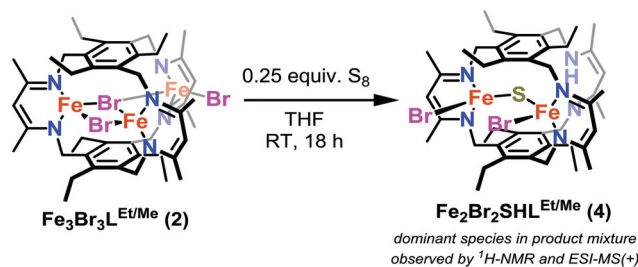


Fig. 4 Non-halide or -sulfide containing  $\text{Fe}_3\text{X}_n$  complexes.

than in the reaction with **2** (Fig. S10–12<sup>†</sup>). To further probe whether the sulfide donor is integral for scrambling or whether such scrambling is a general feature of all multiiron complexes in our ligand, we evaluated scrambling reactions between two of the three complexes  $\text{Fe}_3\text{H}_3\text{L}^{\text{Et/Me}}$ ,  $\text{Fe}_3(\text{NH}_2)_3\text{L}^{\text{Et/Me}}$ , and  $\text{Fe}_3(\text{OME})_3\text{L}^{\text{Et/Me}}$ . In these reactions involving complexes without a sulfide donor, we do not observe evidence ligand exchange, implying that the sulfide is critical to the rapid and facile ligand and electron redistribution observed here. Additionally, scrambling **2** with  $\text{Fe}_3\text{H}_3\text{L}^{\text{Et/Me}}$  exhibited a much slower reaction rate as compared to the analogous reaction using **1** and  $\text{Fe}_3\text{H}_3\text{L}^{\text{Et/Me}}$  showing mostly unreacted starting materials after 48 h, further suggesting that the sulfide donors play a critical role in the reactivity observed (Fig. S15<sup>†</sup>).

The iron centers in all complexes evaluated thus far are four-coordinate with the solid-state structures of the trihydride, triamide, and trimethoxide having hexagonal  $\text{Fe}_3\text{X}_3$  cores whereas that for **2** contains a distorted ladder-like arrangement of the Fe–Br bonds (Fig. 4). The ladder-like structure may allow for more facile approach to one of the Fe centers as the cleft formed by the two Et groups on the lower and upper arene rings and the two  $\beta$ -diketiminato arms is not occupied by a halide donor. We postulated that access to coordination sites on the partner complex might correlate with sulfide transfer/loss from **1**. Reaction of  $\text{Fe}_3\text{NL}^{\text{Et/Me}}$ —each Fe center is three-coordinate—with **1** rapidly afforded a complex mixture of products with complete consumption of both of the starting species.<sup>19</sup> Although identification of specific products from this reaction remains unresolved, the loss of both starting materials is consistent with scrambling and the need for accessible metal coordination sites for exchange.

Having investigated reaction of **1** with various triiron cyclophanate compounds, we then explored pathways to generate diiron complexes from **1** and **3**. We supported the identity of **4** by inducing demetallation of **2** upon reaction with 0.25 equiv. of  $\text{S}_8$  to generate complex **4** as the major species in the product mixture (Scheme 1). The composition of **4** is supported by ESI-MS data wherein ions with  $m/z$  values and isotopic pat-

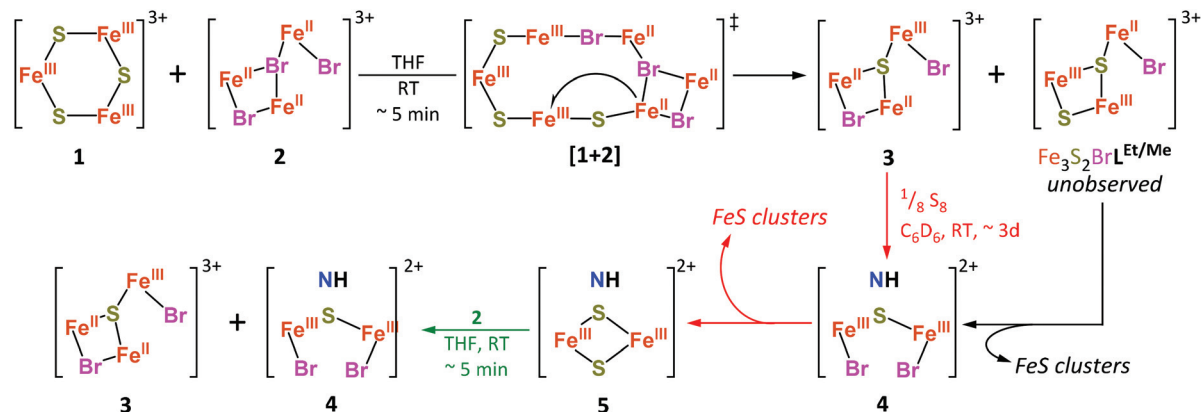


Scheme 1 Alternate route to generate **4**.

terns corresponding to  $m/z$  values for  $[\text{Fe}_2\text{Br}_2\text{SHL}^{\text{Et/Me}} + \text{H}]^+$  are readily observed along with unreacted  $\text{Fe}_3\text{Br}_3\text{L}^{\text{Et/Me}}$  and  $\text{Fe}_3\text{SBr}_2\text{L}^{\text{Et/Me}}$  (Fig. S19 and 20<sup>†</sup>). Although our attempts to refine the synthetic procedure to isolate **4** are ongoing, we were able to obtain single crystals of sufficient quality to determine the connectivity of **4** (Fig. S22<sup>†</sup>). The  $^1\text{H-NMR}$  spectrum of the crystalline material displays the same 10-line spectrum—corresponding to a  $C_{2v}$  symmetric species—as observed in the scrambling product mixture formed between **1** and **2**. The observed structure agrees with the solution-averaged  $C_{2v}$  symmetry based on  $^1\text{H-NMR}$  spectra (Fig. S17<sup>†</sup>).

Armed with the purported  $^1\text{H-NMR}$  resonances for **4**, we then examined whether controlled demetallation of **3** could be effected. Reaction of  $\text{Fe}_3\text{SBr}_2\text{L}^{\text{Et/Me}}$  with elemental sulfur results in a similar outcome as for **2** wherein **3** is consumed to afford **4**. Monitoring this reaction by  $^1\text{H-NMR}$  spectroscopy over 9 days revealed an initial formation of **4** within minutes of mixing at ambient temperature. Resonances assigned to **4** maximize after  $\sim 72$  h while those for **3** decrease and are ultimately no longer observable. Surprisingly, the reaction mixture further evolves with consumption of **4** to generate an additional diiron species,  $\text{Fe}_2(\mu\text{-S})_2\text{HL}^{\text{Et/Me}}$  (**5**), which was not observed in our initial reaction of **1** and **2** (Scheme 2).

Complex **5** was isolated in good yield by reaction of  $\text{Fe}_3\text{H}_3\text{L}^{\text{Et/Me}}$  with excess  $\text{S}_8$  in THF at room temperature to yield  $\text{Fe}_2\text{S}_2\text{HL}^{\text{Et/Me}}$  (**5**) (73%). The composition is corroborated by HR-ESI/MS(+), and the solution  $C_{2v}$  symmetry based on  $^1\text{H-NMR}$  data is consistent with the single crystal X-ray diffraction solution (Fig. 5). From the solid-state structure, the  $[\text{2Fe-2S}]^{2+}$  ferredoxin core is ligated by two nacnac arms ( $\tau'_4$  for each Fe = 0.89 and 0.92) with the third nacnac arm being demetallated. The Fe–S bond metrics and Fe–Fe distances of 2.172(1)–2.209(1) and 2.668(1) Å, respectively, are comparable to the nacnac-supported 2Fe–2S from Holland and coworkers.<sup>21</sup> Notable differences, however, are the longer Fe–N bond lengths (2.017–2.020 Å) and more acute S–Fe–S bond angles (104.82 and 104.98°) in  $\text{Fe}_2\text{S}_2\text{HL}^{\text{Et/Me}}$ , arising from geometric constraints enforced by the cyclophanate scaffold.<sup>22</sup> The IR absorption at  $\sim 1616\text{ cm}^{-1}$  is comparable to one in  $\text{H}_3\text{L}^{\text{Et/Me}}$ , which is lost upon deprotonation, suggesting that the demetallated nacnac is protonated (Fig. S24<sup>†</sup>). Zero-applied field Mössbauer spectra collected on **5** at 80 K display a single quadrupole doublet, which is well simulated with  $\delta = 0.30\text{ mm s}^{-1}$  and  $\Delta E_Q = 0.80\text{ mm s}^{-1}$ . The isomer shift and quadrupole



**Scheme 2** Reactions of 1 with 2 and proposed intermediate and interconversion of 4 and 5.

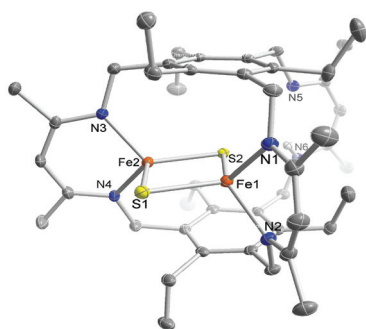


**Fig. 5** ORTEP representation (50% probability) of 5. H atoms and guest solvent molecules have been omitted for clarity. One H atom has been included to depict the reprotonation of the demetallated NACNac chelate. Fe, S, N, and C atoms are depicted as orange, yellow, blue and grey ellipsoids, respectively.

splitting values for 5 are similar to those reported for  $\text{Fe}_3\text{S}_3\text{L}^{\text{Et/Me}}$  (*viz.* 0.30 and 0.29  $\text{mm s}^{-1}$ , respectively).<sup>14</sup> Considering the data in their entirety and the absence of a counter cation in the lattice, we surmise that 5 is comprised of two formally iron (iii) centers and a  $\beta$ -diketimine arm. The comparable Mössbauer parameters as for  $\text{Fe}_3\text{S}_3\text{L}^{\text{Et/Me}}$  suggest the protonated nacnac arm has minimal effect on the cluster electronics.

Formation of 5 in the synthesis of 4 suggests that residual S species either derived from  $\text{S}_8$  or incorporated in ill-defined FeS clusters or aggregates produced by demetallation are capable of reacting with 4 to yield 5. This hypothesis was readily supported; addition of  $\text{S}_8$  to a mixture consisting primarily of 4 generates 5 as the major product with consumption of 4. Decomposition of the  $[\text{3Fe-3S}]^{3+}$  cluster in 1 to afford the  $[\text{2Fe-2S}]^{2+}$  cluster in 5 agrees with the wealth of synthetic reports wherein  $[\text{2Fe-2S}]$  and  $[\text{4Fe-4S}]$  clusters spontaneously assemble from simple precursors and evidence the stability of these clusters under various reaction conditions.<sup>4,5</sup> However, reaction of  $\text{Fe}_3\text{Br}_3\text{L}^{\text{Et/Me}}$  (2) with  $\text{Fe}_2\text{S}_2\text{HL}^{\text{Et/Me}}$  (5) results in complete consumption of 5 and formation of 3 and 4 (Fig. S27†).

Ligand exchange involving the  $[\text{2Fe-2S}]$  cluster in 5 leads us to partly re-evaluate an interpretation based on certain cluster nuclearities as thermodynamic sinks in FeS chemistry. Indeed, two aspects unique to these clusters are the geometric constraints enforced and the templated support offered by the supporting macrobicycle. Arguably, our observations here fail to account for formation of the unknown FeS species generated as a result of demetallation, which are integral to the overall thermodynamic picture. Despite this deficiency, we again lean on prior work in which little if any observed cluster degradation has been reported in synthetic FeS clusters.<sup>1–5</sup> One hypothesis is that such decomposition requires a balance of electron donation to one Fe center concomitant with Fe–S bond cleavage and a Lewis acid to coordinate to the otherwise dangling sulfide. Here then, the reaction partner provides the ideal geometry to favor observed sulfide, electron, and ligand transfers. In the context of dissociation of the belt sulfides from the nitrogenase cofactors, we posit that Fe–S–Fe or Fe–SH–Fe bond-opening and dinitrogen binding may be temporally linked. Such considerations rationalize the proposed ENDOR structures for  $E_4$  with the crystallographic results from Rees and Einsle and their respective coworkers.<sup>22–25</sup> The bond metrics for the FeS cores in 1 and 5 are within the ranges of the wealth of reported  $[\text{2Fe-2S}]$  clusters, suggesting that structural perturbations do not account for the observed reactivity. Finally, we cannot exclude that the stability conferred by our ligand as compared to prior reported systems may allow for isolation and characterization of what might best be described as products from cluster degradation.

We propose the following mechanism for the initial transfer of  $\text{S}^{2-}$  between complexes. First,  $\text{Fe}_3\text{Br}_3\text{L}^{\text{Et/Me}}$  ( $E_{1/2}(\text{2}/\text{2}^+) \sim 0.75$  V vs.  $\text{Fc}/\text{Fc}^+$ ) is not competent to reduce  $\text{Fe}_3\text{S}_3\text{L}^{\text{Et/Me}}$  ( $E_{1/2}(\text{1}/\text{1}^-) = -1.55$  V vs.  $\text{Fc}/\text{Fc}^+$ ), implying that outer-sphere electron transfer does not precede sulfide exchange.<sup>14,15</sup> Second, scrambling from  $\text{Fe}_3\text{S}_3\text{L}^{\text{Et/Me}}$  seemingly requires a bis-cyclophane intermediate insofar as scrambling is only observed between cyclophane complexes. In our mechanism, the first  $\text{S}^{2-}$  transfer from 1 to 2 occurs with  $\text{Br}^-$  transfer yielding 3 and a transient  $\text{Fe}_3\text{S}_2\text{BrL}^{\text{Et/Me}}$  through an inner sphere mechanism similar to

those first discussed by Taube and Endicott (Scheme 2).<sup>26</sup> Decomposition of  $\text{Fe}_3\text{S}_2\text{BrL}^{\text{Et/Me}}$  is a possible pathway to  $\text{Fe}_2\text{SBr}_2\text{HL}^{\text{Et/Me}}$  and **5** with liberation of ill-defined FeS species. Reaction of **3** with  $\text{S}_8$  to generate **4** and ultimately **5** is consistent with the instability of a possible bromido-di( $\mu$ -sulfido) triiron complex.

## Conclusions

In conclusion, we report the reaction of two FeS clusters,  $\text{Fe}_3\text{S}_3\text{L}^{\text{Et/Me}}$  (**1**) and  $\text{Fe}_2\text{S}_2\text{HL}^{\text{Et/Me}}$  (**5**), in which ligand and electron exchange occurs readily with our triiron(II) complexes. This example of Fe–S bond cleavage yields a complex mixture of products wherein two products were assigned as the mixed-ligand species  $\text{Fe}_3\text{Br}_2\text{SL}^{\text{Et/Me}}$  (**3**) and  $\text{Fe}_2\text{Br}_2\text{SHL}^{\text{Et/Me}}$  (**4**), consistent with a ligand exchange reaction. Clean production and subsequent characterization of **4**, precludes an absolute assignment, although the provided characterization data suggest the assignment is reasonable. The results of the indisputable formation of **3** described provide new insight into the lability of FeS clusters under various reaction conditions.

## Conflicts of interest

There are no conflicts to declare.

## Acknowledgements

L. J. M. and W. R. B. acknowledge the National Institutes of Health (R01-GM123241). Mass spectrometry data were collected by the University of Florida Mass Spectrometry Research and Education Center on instrumentation purchased with an award from the National Institutes of Health (S10 OD021758-01A1). The content is solely the responsibility of the authors and does not necessarily represent the official views of the National Institutes of Health. R. G. S. acknowledges Labex ARCANÉ (ANR-11-LABX-0003-01).

## References

- (a) T. Herskovitz, B. A. Averill, R. H. Holm, J. A. Ibers, W. D. Phillips and J. F. Weiher, *Proc. Natl. Acad. Sci. U. S. A.*, 1972, **69**, 2437; (b) B. A. Averill, T. Herskovitz, R. H. Holm and J. A. Ibers, *J. Am. Chem. Soc.*, 1973, **95**, 3523.
- M. A. Bobrik, E. J. Laskowski, R. W. Johnson, W. O. Gillum, J. M. Berg, K. O. Hodgson and R. H. Holm, *Inorg. Chem.*, 1978, **17**, 1402.
- R. W. Johnson and R. H. Holm, *J. Am. Chem. Soc.*, 1978, **100**, 5338.
- (a) L. Deng and R. H. Holm, *J. Am. Chem. Soc.*, 2008, **130**, 9878; (b) S. C. Lee, W. Lo and R. H. Holm, *Chem. Rev.*, 2014, **114**, 3579.
- (a) K. Tanifuji, S. Tajima, Y. Ohki and K. Tatsumi, *Inorg. Chem.*, 2016, **55**, 4512; (b) Y. Ohki and K. Tatsumi, *Z. Anorg. Allg. Chem.*, 2013, **639**, 1340.
- P. Dinis, D. L. M. Suess, S. J. Fox, J. E. Harmer, R. C. Driesener, L. De La Paz, J. R. Swartz, J. W. Essex, R. D. Britt and P. L. Roach, *Proc. Natl. Acad. Sci. U. S. A.*, 2015, **112**, 1362.
- T. Spatzal, K. A. Perez, J. B. Howard and D. C. Rees, *eLife*, 2015, **4**, e11620.
- T. Spatzal, K. A. Perez, O. Einsle, J. B. Howard and D. C. Rees, *Science*, 2014, **345**, 1620.
- (a) D. Sippel and O. Einsle, *Nat. Chem. Biol.*, 2017, **13**, 956; (b) D. Sippel, M. Rohde, J. Netzer, C. Trncik, J. Gies, K. Grunau, I. Djurdjevic, L. Decamps, S. L. A. Andrade and O. Einsle, *Science*, 2018, **359**, 1484.
- W. Kang, C. C. Lee, A. J. Jasniewski, M. W. Ribbe and Y. Hu, *Science*, 2020, **368**, 1381.
- I. Dance, *Dalton Trans.*, 2019, **48**, 1251.
- J. B. Varley, Y. Wang, K. Chan, F. Studt and J. K. Nørskov, *Phys. Chem. Chem. Phys.*, 2015, **17**, 29541.
- I. Čorić, B. Q. Mercado, E. Bill, D. J. Vinyard and P. L. Holland, *Nature*, 2015, **526**, 96.
- Y. Lee, I.-E. Rang, K. A. Abboud, R. García-Serres, J. Shearer and L. J. Murray, *Chem. Commun.*, 2016, **52**, 1174.
- G. L. Guillet, F. T. Sloane, D. M. Ermert, M. W. Calkins, M. K. Peprah, E. S. Knowles, E. Čižmár, K. A. Abboud, M. W. Meisel and L. J. Murray, *Chem. Commun.*, 2013, **49**, 6635.
- Y. Lee, K. A. Abboud, R. García-Serres and L. J. Murray, *Chem. Commun.*, 2016, **52**, 9295.
- Y. Lee, K. J. Anderton, F. T. Sloane, D. M. Ermert, K. A. Abboud, R. García-Serres and L. J. Murray, *J. Am. Chem. Soc.*, 2015, **137**, 10610.
- Y. Lee, F. T. Sloane, G. Blondin, K. A. Abboud, R. García-Serres and L. J. Murray, *Angew. Chem., Int. Ed.*, 2015, **54**, 1499.
- R. B. Ferreira, B. J. Cook, B. J. Knight, V. J. Catalano, R. García-Serres and L. J. Murray, *ACS Catal.*, 2018, **8**, 7208.
- S. R. Alvarado, I. A. Shortt, H.-J. Fan and J. Vela, *Organometallics*, 2015, **34**, 4023.
- M. E. Reesbeck, M. M. Rodriguez, W. W. Brennessel, B. Q. Mercado, D. Vinyard and P. L. Holland, *J. Biol. Inorg. Chem.*, 2015, **20**, 875.
- T. Spatzal, J. Schleiser, E.-M. Burger, D. Sippel, L. Zhang, S. L. A. Andrade, D. C. Rees and O. Einsle, *Nat. Commun.*, 2016, **7**, 10902.
- (a) R. Y. Igarashi, P. C. Dos Santos, W. G. Niehaus, I. G. Dance, D. R. Dean and L. C. Seefeldt, *J. Biol. Chem.*, 2004, **279**, 34770; (b) P. C. Dos Santos, S. M. Mayer, B. M. Barney, L. C. Seefeldt and D. R. Dean, *J. Inorg. Biochem.*, 2007, **101**, 1642; (c) B. M. Barney, D. Lukoyanov, R. Y. Igarashi, M. Laryukhin, T.-C. Yang, D. R. Dean, B. M. Hoffman and L. C. Seefeldt, *Biochemistry*, 2009, **48**, 9094; (d) B. M. Hoffman, D. Lukoyanov, Z.-Y. Yang, D. R. Dean and L. C. Seefeldt, *Chem. Rev.*, 2014, **114**, 4041.
- (a) V. Hoeke, L. Tociu, D. A. Case, L. C. Seefeldt, S. Raugie and B. M. Hoffman, *J. Am. Chem. Soc.*, 2019, **141**, 11984;

- (b) D. Lukoyanov, M. D. Krzyaniak, D. R. Dean, M. R. Wasielewski, L. C. Seefeldt and B. M. Hoffman, *J. Phys. Chem. B*, 2019, **123**, 8823.
- 25 (a) O. Einsle, F. A. Tezcan, S. L. A. Andrade, B. Schmid, M. Yoshida, J. B. Howard and D. C. Rees, *Science*, 2002, **297**, 1696; (b) T. Spatzal, M. Aksoyoglu, L. Zhang, S. L. A. Andrade, E. Schleicher, S. Weber, D. C. Rees and O. Einsle, *Science*, 2011, **334**, 940.
- 26 (a) J. F. Endicott and H. Taube, *J. Am. Chem. Soc.*, 1962, **84**, 4984; (b) J. F. Endicott and H. Taube, *Inorg. Chem.*, 1965, **4**, 437.